A Versatile Method To Prepare RAFT Agent Anchored Substrates and the Preparation of PMMA Grafted Nanoparticles

Chunzhao Li,[†] Junwon Han,[‡] Chang Y. Ryu,*[,†] and Brian C. Benicewicz*[,†]

NYS Center for Polymer Synthesis, Department of Chemistry and Chemical Biology, Department of Chemical and Biological Engineering, Rensselaer Polytechnic Institute, Troy, New York 12180

Received September 12, 2005; Revised Manuscript Received February 25, 2006

ABSTRACT: Well-defined polymer brushes grafted onto silica nanoparticles were prepared by reversible addition−fragmentation chain transfer polymerization (RAFT). A versatile RAFT agent, 4-cyanopentanoic acid dithiobenzoate (CPDB), was attached to amino-functionalized colloidal silica nanoparticles by direct condensation of the mercaptothiazoline-activated CPDB with the surface amino groups. RAFT polymerizations were then conducted from the particle surface to graft polymer brushes to the particles. The kinetics of methyl methacrylate and styrene surface RAFT polymerizations were investigated and compared with model polymerizations mediated by free CPDB. The MMA surface graft polymerization was more controlled than the solution polymerization mediated by free RAFT agent, indicated by the faster polymerization rate and narrower polydispersity. High-performance liquid chromatography techniques were used to quantitatively estimate the amount of ungrafted free polymer which was minimal compared with the grafted polymer.

Introduction

Controlled radical polymerization (CRP) techniques such as atom transfer radical polymerization (ATRP) and nitroxide-mediated polymerization (NMP) have been used widely to prepare polymer grafted substrates by first anchoring an initiator species to the substrates and then initiating polymerization from the substrates.[1−6] Various polymers such as poly(methyl methacrylate) (PMMA), polystyrene (PSt) and poly(*n*-butyl acrylate) (PnBuA) have been successfully grafted from silicates, gold, and CdSe nanoparticles. More recently, reversible addition−fragmentation chain transfer (RAFT) polymerization has been developed as a CRP technique. The mechanism for RAFT polymerization is believed to involve a series of chain transfer reactions (Scheme 1). In the early stages of the polymerization, the addition of a propagating radical (either primary radical or polymeric radical) to the RAFT agent (**1**) is followed by fragmentation of the initial intermediate RAFT radical (**2**) to form a new RAFT agent and release a R• radical, which then reinitiates the polymerization to form additional propagating radicals. The core step of RAFT polymerization is the equilibrium between propagating radicals Pm•, Pn•, and dormant polymeric RAFT agents via the intermediate macro-RAFT radical (**3**). A fast equilibrium is necessary for all the polymeric radicals to propagate with the same probability and achieve low-polydispersity polymers.

Because of the capability to control the polymerization of a wide variety of monomers without using metal catalysts and the mild reaction conditions, RAFT polymerization has received increasing attention. However, the applications of this versatile RAFT technique to prepare polymer grafted substrates are unproportionally meager compared with the large number of reports of RAFT polymerizations in solution,[7−11] probably because of the difficulty to covalently attach RAFT agents to a substrate. Of the very few reports,[13−16] RAFT agent anchored nanoparticles were prepared either by coordination of RAFT agents to nanoparticles[15,16] or by an indirect method via an atom radical transfer addition reaction.[14] Polymer grafted nanoparticles were also prepared by using nanoparticles with anchored AIBN moieties in the presence of free RAFT agents and monomers.[13] The grafted polymers were reported to have low polydispersities. Nevertheless, there are many fundamental questions yet to be answered for RAFT polymerizations on particle surfaces. What are the differences in kinetics of RAFT polymerization on particle surfaces and in solution? How does the RAFT agent surface density affect the polymerization? What is the fraction of ungrafted polymer derived from the AIBN initiator? These questions were partially answered in our recently reported work.[17] In this recent work, RAFT-silane agents were first prepared and covalently attached to silica nanoparticles. Excellent control was demonstrated over the surface graft polymerization of styrene and *n*-butyl acrylate with the RAFT agent anchored silica nanoparticles. Of particular interest was the retardation observed for the surface graft polymerization of styrene and *n*-butyl acrylate, which was ascribed to the localized high RAFT agent concentration near the particle surface. Preliminary results indicated that the fraction of ungrafted polymer was small.

Herein, a versatile route is reported for preparing RAFT agent anchored silica nanoparticles. Silica nanoparticles were first coated with aminosilane agents. A carboxylic acid containing RAFT agent, 4-cyanopentanoic acid dithiobenzoate (CPDB), was activated with 2-mercaptothiazoline. CPDB anchored silica nanoparticles were then prepared by a coupling reaction between the amino-functionalized nanoparticles and the activated CPDB. The kinetics of MMA and styrene surface graft polymerization were investigated and compared with the RAFT polymerization kinetics in solution mediated with free CPDB. HPLC and SEC techniques were used to quantitatively estimate the contents of ungrafted polymers from the as-prepared polymer grafted nanoparticles.

Experimental Section

Materials. Dicyclohexylcarbodiimide (99%), (dimethylamino)-pyridine (99%), and 2-mercaptothiazoline (98%) were purchased from Acros. Aminopropyldimethylethoxysilane (95%) was pur-

[†] NYS Center for Polymer Synthesis, Department of Chemistry and Chemical Biology.

[‡] Department of Chemical and Biological Engineering.

10.1021/ma051983t CCC: $33.50
Published on Web 04/01/2006

Scheme 1. General Reversible Addition−Fragmentation Chain Transfer Polymerization Mechanism

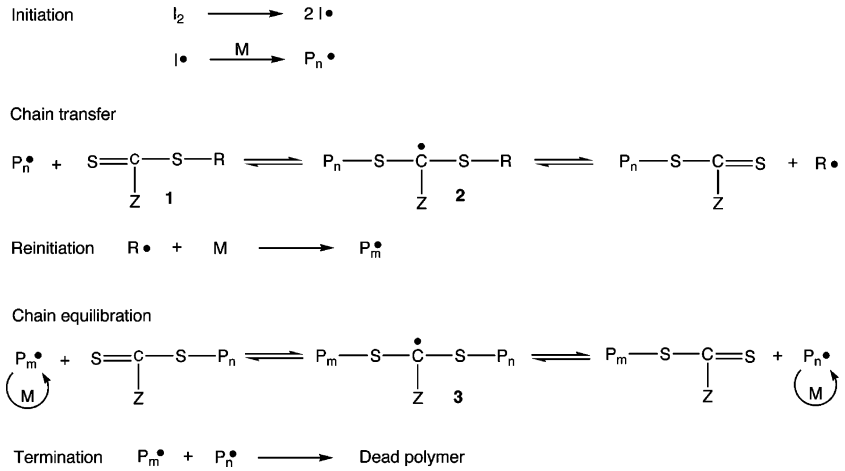

chased from Gelest. Tetrahydrofuran (99.9%, Acros) was dried over CaH_2 overnight and distilled before use. Styrene (99%, Acros) and methyl methacrylate (99%, Acros) were passed through a basic alumina column to remove inhibitor and distilled under vacuum before use. Colloidal silica particles of 30 wt % dispersed in methyl ethyl ketone were kindly provided by Nissan Chemical. The average particle diameter, D_{SiO_2}, was 14 ± 4 nm as measured by TEM and 20 nm as measured by light scattering. Unless otherwise specified, all chemicals were used as received.

Instrumentation. NMR spectra were recorded on a Varian 500 spectrometer using $CDCl_3$ and deuterated DMSO as solvents. FT-IR spectra were recorded using a BioRad Excalibur FTS3000. UV−vis absorption spectra were taken on a Perkin-Elmer Lamda 4C UV/vis spectrophotometer. Molecular weights and molecular weight distributions were determined using a Waters size exclusion chromatograph equipped with a 515 HPLC pump, 2410 refractive index detector, and three Styragel columns (HR1, HR3, and HR4 in the effective molecular weight range of 100−5000, 500−30 000 and 5000−500 000, respectively) with THF as eluent at 30 °C and a flow rate of 1.0 mL/min. The SEC system was calibrated with polystyrene and PMMA standards obtained from Polymer Labs. Analyses of the as-prepared product of the graft polymerization were conducted using two types of HPLC systems. The first was a Waters size exclusion chromatograph equipped with a 515 HPLC pump, a 2410 refractive index detector, and two Styragel columns (HR3 and HR4 in the effective molecular weight range of 500−30 000 and 5000−500 000, respectively) with THF as eluent at room temperature and a flow rate of 0.3 mL/min. The second HPLC system was equipped with a series 1500 pump (Lab Alliance), a UV detector (Acutect-500, λ = 235 nm), and a C18-bonded silica (Zorbax, SB-C18; 150 × 4.6 mm, 5 μm particle, 10 nm pore) packed column with THF as eluent at room temperature and a flow rate of 1 mL/min. HPLC samples were prepared by dissolving the as-prepared PMMA-*g*-SiO_2 samples in pure THF at the concentration of 5 mg/mL and injected at a volume of 20 μL. Calibration of the UV detector signal at λ = 235 nm to quantify PMMA weight for the given 20 μL solution injection was performed using a series of predetermined concentrations of a PMMA homopolymer (M_w = 38K, PDI = 1.05) dissolved in THF.

Synthesis of CPDB. The synthesis of 4-cyanopentanoic acid dithiobenzoate, **4**, was carried out according to the methods in the literature.[12]

Activation of CPDB. CPDB (1.40 g, 5.00 mmol), 2-mercaptothiazoline (0.596 g, 5.00 mmol), and dicyclohexylcarbodiimide (DCC) (1.24 g, 6.00 mmol) were dissolved in 20 mL of dichloromethane. (Dimethylamino)pyridine (DMAP) (61 mg, 0.50 mmol) was added slowly to the solution, which was stirred at room temperature for 6 h. The solution was filtered to remove the salt. After removal of solvent and silica gel column chromatography (5:4 mixture of hexane and ethyl acetate), activated CPDB, **5**, was obtained as a red oil (1.57 g, 83% yield).^{1}H NMR (500 MHz, $CDCl_3$): δ (ppm) 7.90 (d, 2H, J = 7.8, aromatic ring), 7.56 (t, 1H, J = 7.8, aromatic ring), 7.38 (t, 2H, J = 7.8, aromatic ring), 4.58 (t, 2H, J = 7.5, NC**H**$_2$CH$_2$S), 3.60−3.66 (m, 2H, (CN)C(CH$_3$)-CH$_2$**CH**$_2$CON), 3.31 (t, 2H, J = 7.5, NCH$_2$*C***H**$_2$S), 2.50−2.56 (m, 2H, (CN)C(CH$_3$)**CH**$_2$CH$_2$CON), 1.95 (s, 3H, (*C***H**$_3$)C(CN)S). ^{13}C NMR (125 MHz, $CDCl_3$): δ (ppm) 226.7 (Ph**C**=S), 201.9 (N**C**=S), 172.6 (**C**=O), 144.9, 133.1, 128.8, 126.9, 118.8 (**C**N), 56.2, 45.9, 34.6, 33.6, 28.6, 24.5. IR (NaCl disk): 1696 (C=O), 1166 (PhC=S), 1046 cm^{-1} (NC=S).

Preparation of Amino-Functionalized Colloidal Silica Nanoparticles. A suspension (20 mL) of 30 wt % colloidal silica particles was added to a three-necked round-bottom flask with 3-aminopropyldimethylethoxysilane (0.50 g, 3.0 mmol) and dried THF (20 mL). The reaction mixture was heated at 85 °C under N_2 protection overnight and then cooled to room temperature. The reaction mixture was precipitated into a large amount of hexanes (500 mL, ACS Reagent). The particles were recovered by centrifugation at 3000 rpm for 15 min. The particles were then redissolved in 20 mL of acetone and reprecipitated in 200 mL of hexanes. The amino-functionalized particles were dispersed directly into 50 mL of THF for subsequent use. An aliquot of the amino-functionalized silica nanoparticles was dried and subjected to thermal gravimetric analysis to determine the amount of silane agent anchored onto the particles (3.9 wt %). A lower surface density amino-functionalized silica nanoparticles (2.2 wt %) was also prepared similarly using 20 mL of colloidal silica particles and 3-aminopropyldimethylethoxysilane (0.24 g).

Preparation of CPDB Anchored Silica Nanoparticles. A THF solution (30 mL) of the high surface density amino-functionalized silica nanoparticles (3.6 g, 4.1%) was added dropwise to a THF solution (30 mL) of activated CPDB (0.50 g, 1.3 mmol) at room temperature. After complete addition, the solution was stirred for 6 h. The reaction mixture was then precipitated into a large amount of 4:1 mixture of cyclohexane and ethyl ether (500 mL). The particles were recovered by centrifugation at 3000 rpm for 15 min. The particles were then redissolved in 30 mL of THF and reprecipitated in 4:1 mixture of cyclohexane and ethyl ether. This dissolution−precipitation procedure was repeated another three times until the supernatant layer after centrifugation was colorless. The high surface density CPDB anchored silica nanoparticles (CPDB-NP-1) were dried at room temperature (3.5 g, 97% yield). The low surface density CPDB anchored silica nanoparticles (CPDB-NP-2) were prepared similarly using a THF solution (30 mL) of the low surface density amino-functionalized silica nanoparticles (3.6 g, 2.2%) and activated CPDB (0.27 g, 0.70 mmol). The purified CPDB-NP-2 had a yield of 95%.

MMA Graft Polymerization from CPDB Anchored Silica Nanoparticles. RAFT agent anchored silica (0.030 g, 131 μmol/g), THF (0.75 mL), and MMA (0.75 mL, 7.0 mmol) were added to a 15 mL Schlenk tube followed by sonication and addition of AIBN (9.0 μL of 0.05 M THF solution). The tubes were subjected

to three cycles of freeze−pump−thaw to remove oxygen. The tubes were then placed in an oil bath preset to 60 °C for various intervals. The polymerizations were stopped by quenching the tubes in ice water, and the polymerization mixtures were poured into an aluminum boat to evaporate the solvent in a fume hood. The aluminum boat was then transferred to a vacuum oven to remove traces of solvent and monomer at 30 °C overnight to determine the monomer conversions via gravimetric analysis. A monomer conversion of 22% was reached after 7 h. The cleaved PMMA had a number-average molecular weight of 37 900 and a PDI of 1.07.

Styrene Graft Polymerization from CPDB Anchored Silica Nanoparticles. RAFT agent anchored silica nanoparticles (0.030 g, 131 μmol/g), THF (0.70 mL), and styrene (0.70 mL, 6.0 mmol) were added to a 15 mL Schlenk tube followed by sonication and addition of AIBN (9.0 μL of 0.05 M THF solution). The tube was subjected to three cycles of freeze−pump−thaw to remove oxygen. The tubes were then placed in an oil bath preset to 65 °C for various intervals. The polymerization was stopped by quenching the tubes in ice water, and the polymerization mixture was poured into an aluminum boat to evaporate the solvent in a fume hood. The aluminum boat was then transferred to a vacuum oven to remove traces of solvent and monomer at 30 °C overnight to determine the monomer conversions via gravimetric analysis. A monomer conversion of 4.8% was reached after 35 h. The cleaved PSt had a number-average molecular weight of 8500 and a PDI of 1.10.

General Procedures for Cleaving Grafted Polymer from Particles. In a typical experiment, 50 mg of PMMA or PSt grafted silica particles was dissolved in 3 mL of THF. Aqueous HF (49%, 0.2 mL) was added, and the solution was allowed to stir at room temperature overnight. The solution was poured into a PTFE Petri dish and allowed to stand in a fume hood overnight to evaporate the volatiles. The recovered PMMA or PSt was then subjected to SEC analyses.

Results and Discussion

Preparation of CPDB Anchored Silica Nanoparticles. In a previous paper, we reported the first preparation of a RAFT-silane agent and its use to prepare RAFT agent anchored silica nanoparticles.[17] The RAFT-silane agent was prepared via a multistep synthesis involving reactions and purifications of intermediates containing methoxysilane groups, which led to a overall low yield of the purified RAFT-silane agent because of the instability of the methoxy group and the absorption of the RAFT-silane agent to the silica gel during column chromatography. PSt, PnBuA, and block copolymer brushes grafted onto silica nanoparticles were successfully prepared by employing the anchored RAFT agents. However, methyl methyacrylate could not be controlled by this anchored RAFT agent. It is thus desirable to develop a simple and versatile method to attach RAFT agents to silica nanoparticles, capable of controlling the polymerization of a wider variety of monomers.

It was reported that the carboxyl group bearing CPDB, **4**, could control the radical polymerization of a variety of monomers (methacrylates, acrylates, styrenics) to provide polymers with predictable molecular weight and narrow polydispersities.[12,18] In the current work, the RAFT agent was attached to silica nanoparticles by reacting the carboxyl group of CPDB with silica nanoparticles bearing appropriate functional groups. Amino group-functionalized silica nanoparticles were first prepared by refluxing 3-aminopropyldimethylethoxysilane with silica nanoparticles. After precipitation into hexanes, the purified amino group anchored silica nanoparticles were redispersed into THF. The selection of reaction conditions to attach CPDB to the amino-functionalized nanoparticles was critical to the success of the approach. Competing reactions or condensation reactions that produced acidic byproducts limited the scope of reactions for the attachment. Attempts to directly

Scheme 2. Synthesis Procedures of 4-Cyanopentanoic Acid Dithiobenzoate Anchored onto Silica Nanoparticles

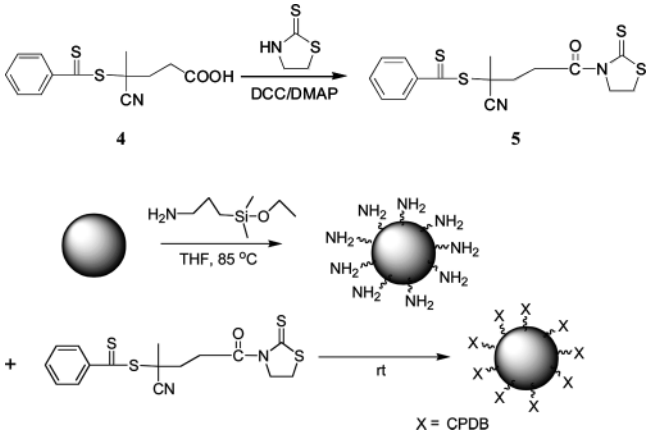

prepare the CPDB anchored silica nanoparticles by reacting the carboxyl group bearing CPDB and amino group of the modified silica nanoparticles with DCC as the condensation agent failed to yield the desired product. It is well-known that dithioesters are susceptible to aminolysis even under mild conditions.[19−21] In fact, a model reaction of CPDB with *n*-butylamine catalyzed by DCC and DMAP failed to yield the desired amide. Instead, the characteristic red color of the dithiobenzoate changed gradually to yellow, indicating aminolysis of the dithiobenzoate group. Therefore, the carboxyl group of CPDB was first activated with 2-mercaptothiazoline.[22] A second model reaction was then conducted to determine whether the reactivity of the mercaptothiazoline activated amide bond is sufficiently high to selectively consume the amino groups in the presence of dithiobenzoate groups. After dropwise addition of *n*-butylamine to the activated CPDB (1:1 mole ratio) and stirring for 2 h, the characteristic red color of the dithiobenzoate was still preserved. Subsequent column chromatography of the products showed that the *n*-butylamine end-capped CPDB and 2-mercaptothiazoline were the only products formed, thus confirming the selectivity of the reaction and preservation of the thiocarbonylthio bond. High and low surface density CPDB anchored silica nanoparticles were thus prepared by the reaction of amino group-functionalized silica nanoparticles and activated CPDB (Scheme 2).

The attachment of CPDB onto silica nanoparticles was confirmed by FT-IR, which revealed the characteristic absorption bands at 2242 and 1450 cm^{-1} due to the cyano group and phenyl ring, respectively. A small absorption attributed to the newly formed amide bond at 1538 cm^{-1} due to N−H bending vibrations was also observed. The thiocarbonyl absorption at 1120 cm^{-1} and carbonyl absorption (amide bond) at 1638 cm^{-1} due to carbonyl bond were not observed due to the overlap with the strong absorption of bare silica and absorbed water. The ^1H NMR spectrum of CPDB anchored silica nanoparticles dispersed in d_6-DMSO also showed the chemical shifts due to the aromatic protons of CPDB at 7.0−8.5 ppm. The attachment of CPDB onto silica nanoparticles was further confirmed by UV−vis spectrometry. The amount of RAFT agent anchored onto the modified silica nanoparticles was determined quantitatively by comparing the absorption at 300 nm for the CPDB anchored silica nanoparticles to a standard absorption curve made from known amounts of the free CPDB.

Kinetics of Surface Graft Polymerization. The CPDB anchored silica nanoparticles used for MMA radical polymerization had surface densities of 131 μmol/g (CPDB-NP-1) and 65 μmol/g (CPDB-NP-2), which is equivalent to 0.54 and 0.27

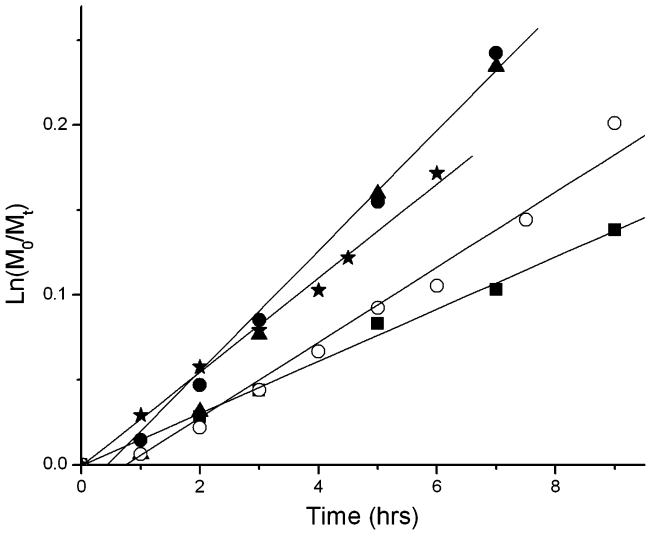

Figure 1. Pseudo-first-order rate plot for the polymerization of methyl methacrylate (4.65 M in THF) with 2,2′-azobis(isobutyronitrile) as initiator (3.0×10^{-4} M) mediated with 4-cyanopentanoic acid dithiobenzoate (CPDB)-functionalized nanoparticles; high surface density (CPDB-NP-1) (2.62×10^{-3} M, solid circle); low surface density (CPDB-NP-2) (2.62×10^{-3} M, solid triangle); without CPDB (solid star); hybrid system (1.31×10^{-3} M, CPDB-NP-1 + 1.31×10^{-3} M free CPDB, open circle); free CPDB (2.62×10^{-3} M, solid square) at 60 °C.

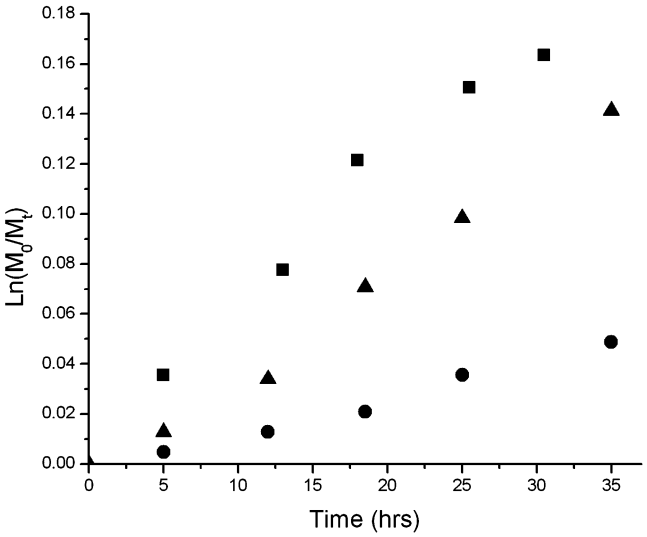

Figure 2. Pseudo-first-order rate plot for the polymerization of styrene (4.3 M in THF) with 2,2′-azobis(isobutyronitrile) as initiator (3.2×10^{-4} M) mediated with 4-cyanopentanoic acid dithiobenzoate (CPDB)-functionalized nanoparticles; high surface density (CPDB-NP-1) (2.8×10^{-3} M, solid circle); low surface density (CPDB-NP-2) (2.8×10^{-3} M, solid triangle circle); free CPDB (2.8×10^{-3} M, solid square) at 65 °C.

RAFT agents/nm^2, respectively, by assuming the density of colloidal silica is comparable to bulk silica (2.07 g/cm^3) and using a similar calculation procedure reported by Pyun et al.[3] For the polymerization of MMA, the molar ratio of [AIBN]/[CPDB] was set to 0.11 to minimize termination by surface anchored polymeric radical recombination due to the reported "enhanced recombination" by the surface radical migration effect.[14] The relatively low [AIBN]/[CPDB] ratio also helped to reduce the amount of free polymer derived from the initiator, AIBN, and yet maintain a moderate polymerization rate. The surface graft polymerizations of MMA mediated by the CPDB anchored silica nanoparticles with the two surface densities were conducted at identical reaction conditions to investigate the effect of RAFT agent surface density on MMA polymerization kinetics. MMA free radical polymerizations in solution mediated with and without free CPDB at identical conditions were also conducted for comparison. Polymerizations were not conducted beyond 9 h since the polymerization mediated with CPDB anchored silica nanoparticles gelled at that time. The CPDB anchored nanoparticles with different surface densities were also employed for styrene surface graft polymerizations. For the same considerations as mentioned above, a low [AIBN]/[CPDB] ratio (0.11) was chosen for all styrene polymerizations.

The results of the kinetics studies for MMA polymerizations mediated by the nanoparticles with the two different CPDB surface densities, free CPDB, and conventional MMA radical polymerization are shown in Figure 1. The graph shows an almost linear relationship between monomer consumption and time for all five cases, which indicates a constant free radical concentration during the polymerization. Surprisingly, the rate of polymerizations mediated by the two surface anchored CPDBs were much higher than the model polymerization mediated by free CPDB at identical conditions. The polymerization rates were even slightly higher than the MMA polymerization without RAFT agents, although these data could be equivalent within the experimental error. A polymerization mediated by 50% free CPDB and 50% CPDB-NP-1 at the identical conditions showed an intermediate rate. This is contrary to current and previously reported results for styrene and *n*-butyl acrylate surface graft polymerizations.[17] The MMA polymerizations mediated by anchored CPDB nanoparticles were also characterized by a slight induction period of ~30 min, whereas inhibition was not observed for the polymerization mediated with free CPDB or without CPDB. Additionally, there were no appreciable differences between the polymerization kinetics of the two anchored CPDB systems, which is again different from the current and previously reported results for styrene polymerization.

For styrene polymerizations mediated with anchored CPDBs and free CPDB, a linear increase in monomer conversion with polymerization time was observed for all three polymerizations (Figure 2). The free CPDB mediated polymerization exhibited the highest apparent polymerization rate, followed by the low surface density anchored CPDB (65 μmol/g) mediated polymerizations which exhibited an intermediate polymerization rate. The high surface density anchored CPDB (131 μmol/g) mediated polymerization showed the lowest rate. This trend is consistent with observations in a previous paper[17] for styrene surface graft polymerization and was ascribed to the "localized high RAFT agent concentration" effect. However, this mechanism does not explain the MMA surface graft polymerization kinetics of the current work in which the rates for polymerization mediated by the anchored CPDBs were higher than for free CPDB. It must also be pointed out that all four MMA polymerizations were conducted at moderate monomer concentration (4.65 M) and stopped at low conversion (<25%), which means polymerization rate acceleration due to gel effects were negligible in these experiments. Therefore, the RAFT polymerization mechanism must be affected by other factors which cause the kinetic effects observed in this work.

In a radical polymerization mediated with either surface anchored RAFT agents or free RAFT agents, the chain propagation events are largely unaffected by the attachment of the RAFT agent. However, the chain transfer reactions are more complicated for the polymerization mediated with surface anchored RAFT agents than with the free RAFT agent. As many as five possible chain transfer modes can be identified (Scheme 3). For

Scheme 3. Chain Transfer Reactions for the Radicals (a) in Solution and (b) on Particle Surface

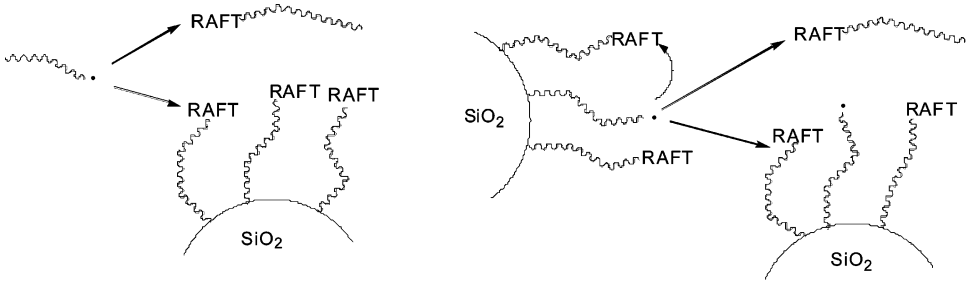

the radicals produced in solution by AIBN decomposition, their fate is predominately the transfer to particle surface after reaction with the surface anchored RAFT agents which will produce a radical on the particle surface and release a free RAFT agent into solution. A second chain transfer mode for the radical in solution is to react with the free RAFT agents transferred to solution by the reaction described above. However, the amount of free RAFT agents transferred into solution should be small because of the low [AIBN]/[CPDB] ratio used, the low initiation efficiency of AIBN, and low conversion range investigated in this work. This chain transfer mode will thus be neglected in the current discussion. For the radical transferred to the particle surface, it could react with a RAFT agent on another particle surface, a RAFT agent in solution, or a neighboring RAFT agent on the same particle surface (Scheme 3b). The first mode requires interpenetration of the surface polymer layers on the two particles which will incur a large entropic barrier; thus, this interparticle chain transfer rate could be very slow. The second mode is expected to be negligible because the experimental conditions used in the current work will produce only a very small amount of RAFT agent in solution, thus leaving the majority of RAFT agents on particle surface. This means that the predominate chain transfer mode of the radical on surface is to react with the neighboring anchored RAFT agents which have a very high local concentration on the surface layer of the particle. Thus, the overall progression of the surface anchored RAFT agent mediated polymerization could thus be envisaged as follows: first, the initiator decomposes to form primary radicals which will directly transfer to particle surface or add a small number of monomer units and then transfer to the particle surface by reacting with the surface anchored RAFT agents; second, most of the surface anchored radicals will remain on the same particle, either propagating through monomer addition or migrating to a neighboring dormant polymeric RAFT agent by a chain transfer reaction via an intermediate macro-RAFT agent radical. The intermediate macro-RAFT radical on the particle surface however is quite different from that in solution. The two polymer chains of the surface anchored intermediate radical are immobilized to the same particle surface whereas the two polymer chains of the intermediate radical in solution are less restricted. This unique confined geometry may contribute to the unusually high rate of MMA surface graft polymerization observed in this work. The only other major characteristic that differentiates the polymerization on the particle surface and in solution is the localized high RAFT agent concentration effect, which would only decrease the rate of polymerization or affect inhibition.

Indeed, as discussed in the literature, slow fragmentation of the initial intermediate radical (**2**) and the intermediate macro-RAFT radical (**3**) are believed to be strongly associated with the inhibition and retardation commonly observed for RAFT polymerization as compared to the polymerization without RAFT agents.[11,23−28] Retardation has been observed for St and methyl acrylate polymerizations mediated by either monomeric RAFT agents or polymeric RAFT agents.[23,29,30] MMA,[18] 4-anilinophenyl acrylate,[31] and phenyl methacrylamide[31] polymerizations mediated with CPDB were also found to be generally slower than the CPDB-free system. Therefore, any factors that destabilize the intermediate macro-RAFT radical will likely increase the fragmentation rate of the intermediate radical and hence the overall polymerization rate. Although the exact reason for the higher polymerization rate of MMA on particle surface is not clear, it is speculated that a combination of the unique confined geometry of the intermediate macro-RAFT radical on particle surface and the bulky structure of MMA monomer may contribute to the destabilization of the PMMA intermediate macro-RAFT radical.

Additional studies were conducted of the RAFT polymerization on particle surfaces and in solution by examining MMA polymerizations mediated by hybrid CPDB agents (50% surface anchored CPDB-NP-1 + 50% free CPDB; see Figure 1) at the identical experimental conditions as described earlier. With the presence of both free and surface anchored CPDBs, the polymerization proceeded both in solution and on the particle surface. The final products were composed of two major species: PMMA-*g*-SiO_2 derived from surface anchored CPDB agents and free PMMA derived from the CPDB in solution. As expected, the polymerization rate was intermediate of the pure anchored CPDB and pure free CPDB systems (Figure 1). Selected SEC traces of the polymer recovered at various polymerization times after treating the polymer grafted silica nanoparticles with HF are shown in Figure 3 (dotted line). Bimodal distributions were observed for the polymerizations. The two peaks of the SEC traces gradually merged as conversion increased, and only one symmetrical peak was observed at 21 h (35% conversion). On the basis of the previous discussion of polymerization rates, it was tempting to assign the high-M_w peak of each trace to the PMMA cleaved from particle surface and the low-M_w peak to the free PMMA since the polymerization rate on the particle surface was higher than in solution. However, it is also important to consider the approximately half-hour induction period for the polymerizations conducted on particle surfaces. For an unequivocal assignment, the as-prepared products were also subjected to SEC analyses. Two peaks could be expected from the SEC traces of these as-prepared samples because of the two major species present in the product: free PMMA with long retention time and very high "equivalent molecular weight" PMMA-*g*-SiO_2 nanoparticles with short retention time. The SEC traces of the as-prepared samples (free polymer and nanoparticles) are also shown in Figure 3 (solid line). The 2 h as-prepared sample showed only one peak which was ascribed to the free PMMA since the very short chain PMMA grafted silica nanoparticles did not dissolve well in THF and were removed by a further filtration before SEC injection.

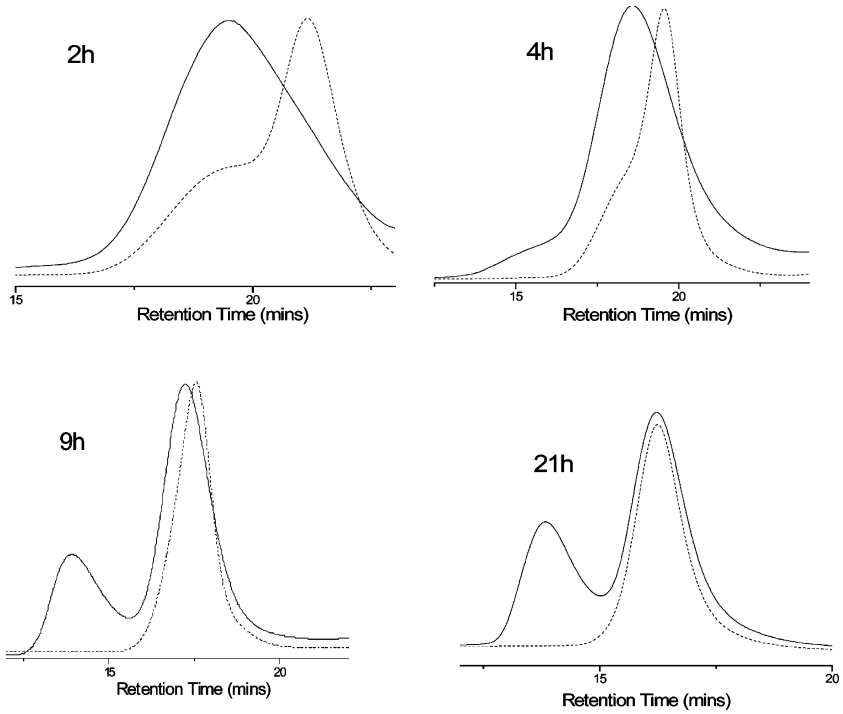

Figure 3. Size exclusion chromatography traces of the as-prepared (solid line) and hydrofluoric acid etched (dash line) products of methyl methacrylate polymerization (4.65 M in THF) with 2,2′-azobis(isobutyronitrile) as initiator (3.0×10^{-4} M) mediated with the hybrid 4-cyanopentanoic acid dithiobenzoate (CPDB) system (1.31×10^{-3} M, high surface density CPDB-NP-1 + 1.31×10^{-3} M free CPDB) at 60 °C.

By comparing the two SEC traces of these 2 h samples, the high-M_w peak of the HF-etched sample could be easily ascribed to the free polymer. For the 4, 9, and 21 h as-prepared PMMA-*g*-SiO_2 samples (Figure 3), bimodal distributions of the SEC traces were indeed observed and ascribed to the free PMMA and PMMA-*g*-SiO_2. By comparing the 4 and 9 h as-prepared samples and HF-etched samples (Figure 3), similarly, the higher molecular weight humps of the HF-etched samples were again ascribed to the free PMMA and the lower molecular weight major peaks to the grafted PMMA cleaved from the particle surfaces, and these two peaks converged with conversion. At even higher conversion (21 h, 35%), the HF-etched sample showed only one symmetrical peak which agreed well with the free PMMA peak of the as-prepared sample. This behavior could be explained by the short induction period of the polymerization on the particle surface which resulted initially in lower initial molecular weights of the grafted PMMA on the particle surfaces. A concurrent higher rate of polymerization on the particle surface resulted in polymer molecular weights on the surface which neared and eventually matched those of the free polymer. Of particular interest is the high molecular weight PMMA-*g*-SiO_2 hump/peak observed in the as-prepared samples. As conversion increased from 6.5% to 18.3% to 35%, the retention time of the PMMA-*g*-SiO_2 gradually decreased from 15.10 to 14.10 to 13.86 min. This is a good qualitative indication that the molecular weight of the PMMA on the particle surfaces gradually increased with conversion, resulting in a gradual increase of hydrodynamic volume of the PMMA-*g*-SiO_2.

The controlled character of MMA graft polymerization was demonstrated by the results presented in Figure 4. These results showed that the number-average molecular weights increased in a linear fashion with monomer conversions, and the measured molecular weights determined by SEC calibrated with PMMA standards were close to theoretical molecular weights (solid line), which indicated a very high efficiency of the anchored CPDB throughout the polymerization. Also interesting is the evolution of the molecular weight distribution of the cleaved

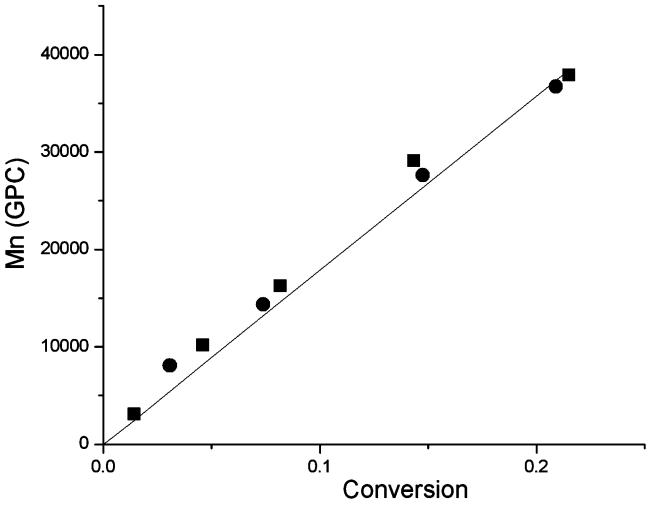

Figure 4. Dependence of number-average molecular weight on conversion for methyl methacrylate polymerization (4.65 M in THF) with 2,2′-azobis(isobutyronitrile) as initiator (3.0×10^{-4} M) mediated with 4-cyanopentanoic acid dithiobenzoate (CPDB)-functionalized nanoparticles, high surface density (CPDB-NP-1) (2.62×10^{-3} M, solid square); low surface density (CPDB-NP-2) (2.62×10^{-3} M, solid circle) at 60 °C.

PMMA. As shown in Figure 5, the polydispersities of PMMA prepared with free CPDB were as high as 1.43 at 2.7% conversion and gradually dropped to 1.16 at 13% conversion. High PDI (1.74−1.29) PMMA prepared at low conversion (1.4%−18%) by a similar RAFT agent 2-cyanoprop-2-yl dithiobenzoate was also reported by Chong et al.[18] Surprisingly, the polydispersities of the cleaved PMMA from PMMA-*g*-SiO_2 prepared by either CPDB-NP-1 or CPDB-NP-2 were significantly narrower than that of the PMMA prepared by free CPDB at lower conversions. For the cleaved PMMA, the polydisperisities were as narrow as 1.14 at the first conversion point (3.2%), dropped to less than 1.1 at 5% conversion, and were less than 1.1 over the reminder of conversion range investigated

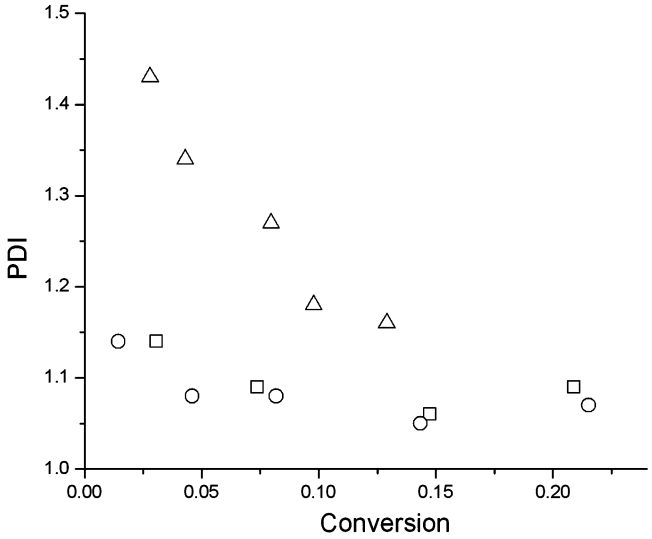

Figure 5. Dependence of polydispersity (PDI = M_w/M_n) on conversion for methyl methacrylate polymerization (4.65 M in THF) with 2,2′-azobis(isobutyronitrile) as initiator (3.0×10^{-4} M) mediated with 4-cyanopentanoic acid dithiobenzoate (CPDB)-functionalized nanoparticles, high surface density (CPDB-NP-1) (2.62×10^{-3} M, open square); low surface density (CPDB-NP-2) (2.62×10^{-3} M, open circle): free CPDB (2.62×10^{-3} M; open circle, open triangle) at 60 °C.

(21.5%). Since polydispersity depends on the chain transfer constant of both initial RAFT agent and polymeric RAFT agent formed during polymerization, this result strongly suggested that the surface anchored CPDB was an even more effective chain transfer agent than the free CPDB in solution. This could be due to a much higher fragmentation rate of the anchored intermediate radical compared with the free intermediate radicals and also a highly effective chain transfer reaction due to the localized high RAFT agent concentration. Thus, most of the R radicals participated in the polymerization at an even earlier stage, and much lower polydispersities were achieved for the surface anchored polymers. For St polymerization, CPDB is already a very excellent chain transfer agent, indicated by the narrow polydispersities and agreement between theoretical and measured molecular weights at very low conversions (Figure 6). Therefore, no appreciable differences of the polydispersity and molecular weights were observed for the surface graft polymerization and polymerization in solution. This work demonstrates that the structure and steric environment of the surface anchored intermediate radical can have a significant effect on RAFT polymerization.

Determination of the Fraction of Ungrafted Polymer. An advantage of using surface anchored RAFT agents on nanoparticles claimed here is that only relatively small amounts of ungrafted polymers will be produced. As the RAFT mechanism indicates, the initiating species for the polymer chains originate from the initiator or R group of the RAFT agent. The amount of polymer derived from initiator is determined largely by the [AIBN]/[RAFT agent] ratio, AIBN initiation efficiency, and monomer conversion. For the polymerization mediated by surface anchored RAFT agents and initiated by AIBN in solution, it is thus possible to obtain polymer grafted nanoparticles free from large amounts of ungrafted free polymer impurities by using a low [AIBN]/[RAFT agent] ratio (~0.1) and controlling the polymerization at a low conversion.

On the basis of the distinct size difference of the PMMA grafted silica nanoparticles ($D_{PMMA-g-SiO_2} \sim 20-50$ nm, measured using dynamic light scattering) and ungrafted PMMA

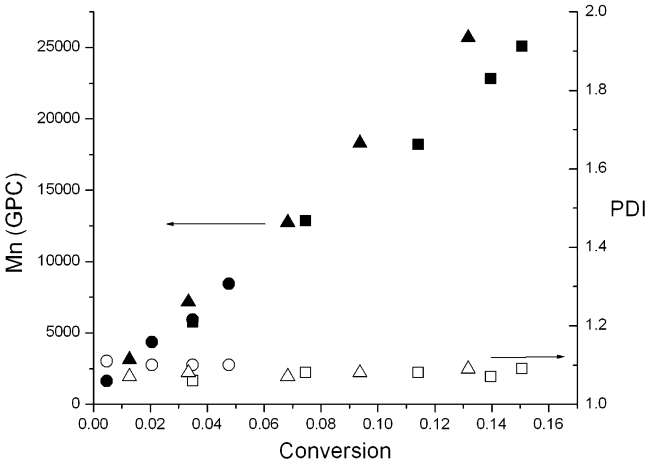

Figure 6. Dependence of number-average molecular weight and polydispersity on conversion for styrene (4.3 M in THF) polymerization with 2,2′-azobis(isobutyronitrile) as initiator (3.2×10^{-4} M) mediated with 4-cyanopentanoic acid dithiobenzoate (CPDB)-functionalized nanoparticles, high surface density (CPDB-NP-1) (2.8×10^{-3} M, square); low surface density (CPDB-NP-2) (2.8×10^{-3} M, circle); free CPDB (2.8×10^{-3} M, triangle) at 65 °C.

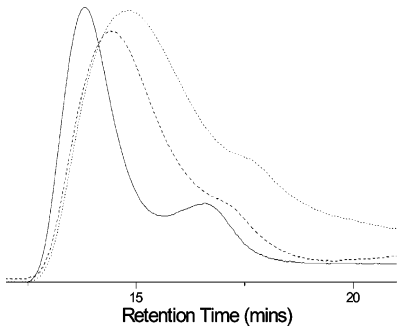

Figure 7. Size exclusion chromatography profiles of the as-prepared PMMA-*g*-SiO_2 at 12% conversion (dotted line, M_n 23 600), 16% conversion (dashed line, M_n 29 100), and 22% conversion (solid line, M_n 39 100).

(R_g < 5 nm), HPLC techniques were employed to analyze the content of ungrafted PMMA in the as-prepared samples which were synthesized by using CPDB-NP-1 as the RAFT agent for the polymerization. Two different types of HPLC columns were used: one was a series of cross-linked polystyrene columns (Waters, Styragel HR 4 and HR 3), and the other was a C18-bonded silica column (Zorbax, SB-C18). Figure 7 shows the SEC profiles of the as-prepared samples at different conversions using the Styragel columns and RI detector. On the basis of the size exclusion mechanism, the peaks at shorter and longer retention times in each SEC trace corresponded to the elution of the larger PMMA-*g*-SiO_2 and the smaller ungrafted PMMA, respectively. The peaks of the ungrafted PMMA and PMMA-*g*-SiO_2 shifted toward smaller retention times upon increasing conversion, suggesting the increase of molecular weights at higher conversion. The peak area of the PMMA-*g*-SiO_2 was apparently much larger than that of the ungrafted PMMA in Figure 7, but the two peaks were not well separated enough to clearly provide quantitative information on the amount of the ungrafted PMMA.

A C18-bonded silica packed column was then used in an attempt to separate the PMMA-*g*-SiO_2 from ungrafted free PMMA. Figure 8 shows the HPLC profiles of a PMMA homopolymer (M_n = 38 000, PDI = 1.05), pure solvent THF, and as-prepared PMMA-*g*-SiO_2 samples at different conversions using a C18-bonded silica column. In contrast to the Styragel SEC profiles, a well-resolved peak prior to the solvent peak

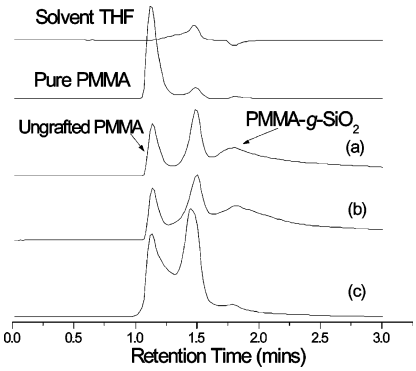

Figure 8. High-performance liquid chromatography profiles of solvent THF, pure free PMMA, and as-prepared PMMA-*g*-SiO_2 samples after conversions of (a) 12%, (b) 16%, and (c) 22%, using C18-bonded silica column (Zorbex SB-C18; 150 × 4.6 mm) packed with the silica particles with 5 μm diameter and 10 nm pores) and THF as eluent.

Table 1. Fraction of Ungrafted Poly(methyl methacrylate) in the As-Prepared PMMA-*g*-SiO_2 at Various Conversions

sample no.	conv (%)	M_n(SEC) (g mol^{-1})	PDI	fraction of ungrafted polymer (wt %)
1	12	23 600	1.06	5.2
2	16	29 100	1.06	5.1
3	22	39 100	1.07	13.4

could be obtained for the as-prepared PMMA-*g*-SiO_2 samples. This peak corresponds to the elution of the ungrafted PMMA in the as-prepared PMMA-*g*-SiO_2, following the similar SEC-like elution of the PMMA homopolymers. Because of the clear separation of ungrafted PMMA peak from PMMA-*g*-SiO_2 using the C18-bonded silica column, we were able to quantify the contents of ungrafted PMMA in as prepared PMMA-*g*-SiO_2. The amount of ungrafted PMMA was determined quantitatively by comparing the ungrafted PMMA peak area using Gaussian fit after calibrating the UV detector signal at $\lambda = 235$ nm using a series of PMMA homopolymers with known concentrations. The results are summarized in Table 1 to show that the amount of ungrafted polymer was generally very low, only around 5 wt % of the total polymer prepared up to 16% conversion and less than 15 wt % of the total polymer prepared at 22% monomer conversion.

In Figure 8, the elution of the PMMA-*g*-SiO_2 occurred as a very broad peak with the C18-bonded silica column, which has an even longer retention time than the elution of solvent THF. This is quite different from the retention behavior of the PMMA-*g*-SiO_2 in the Styragel column. We speculate that the distinct difference of retention behavior of PMMA-*g*-SiO_2 between polymer-based and silica-based columns originates from the rigidity of HPLC packing materials for the polymer separation. Because the PMMA-*g*-SiO_2 has a hard silica core, the deformability of the stationary phase will significantly affect its retention during HPLC. We designate the polymer-based SEC column as a "soft" SEC column because swollen cross-linked polystyrene gels in THF are deformable during the permeation of PMMA-*g*-SiO_2 through the SEC column. Such flexibility of the "soft" column can offer the size-based SEC separation regardless of the free PMMA or PMMA-*g*-SiO_2. In contrast, the C18-bonded nanoporous silica particles are "rigid" packing materials, which cannot be deformed upon the permeation of PMMA-*g*-SiO_2 during HPLC. While the free PMMA still exhibits the typical SEC-like retention behavior (elution before solvent peak), the PMMA-*g*-SiO_2 particles are eluted as a very broad peak with a peak maximum after the elution of the solvent peak, when the C18-bonded silica column is used (Figure 8). This delayed elution may be due to the possible polar/polar attractive interactions of silica surfaces between the PMMA grafted nanoparticle cores and nanoporous C18-silica packing materials.

Conclusions

In this work, it was demonstrated that CPDB anchored silica nanoparticles could be easily prepared by the reaction of the carboxyl group activated CPDB with amino-functionalized silica nanoparticles. The kinetics of MMA and St surface graft polymerizations mediated by CPDB anchored silica nanoparticles with two different surface densities were investigated and compared with the free CPDB mediated polymerization. It was found that the surface anchored CPDB showed excellent control over the surface graft polymerization of MMA and styrene. The rate of MMA surface graft polymerization mediated by the anchored CPDB was much higher than the polymerization mediated by free CPDB. Polydispersities of the PMMA cleaved from the particle surface were much narrower than the PMMA prepared using free CPDB as the RAFT agent. The polymerization behavior was attributed to the unique structure and steric environment of the surface anchored intermediate macro-RAFT agent radical and also the localized high RAFT agent concentration effect. Polymerizations mediated by a hybrid CPDB system (free RAFT agent plus RAFT agent anchored onto silica nanoparticles) showed that the free polymer had a higher initial molecular weight than the grafted polymer which converged at high conversions. Two types of HPLC equipped with Styragel columns or a C18-coated silica column were used to separate the ungrafted PMMA polymer from the PMMA-*g*-SiO_2. It was found that the PMMA-*g*-SiO_2 followed the normal size exclusion mechanism for elution from soft Styragel columns. On the contrary, it was eluted as broad peak from a rigid silica column, possibly due to entrapment and gradual elution from the rigid silica column. Using our surface anchored RAFT agent, we were able to minimize the amount of ungrafted PMMA polymer in the as-prepared PMMA-*g*-SiO_2 (5 and 15 wt % for 16% and 22% monomer conversion, respectively.)

Acknowledgment. The authors thank Eastman Kodak Co. for their generous financial support through the Nanoscale Science and Engineering Initiative of the National Science Foundation under NSF Award DMR-0117792. C.Y.R. also gratefully acknowledges receipt of a NSF CAREER Award, #0447936.

References and Notes

(1) Werne, T. V.; Patten, T. E. *J. Am. Chem. Soc.* **2001**, *123*, 7497−7505.
(2) Ohno, K.; Koh, K.; Tsujii, Y.; Fukuda, T. *Macromolecules* **2002**, *35*, 8989−8993.
(3) Pyun, J.; Jia, S.; Kowalewski, T.; Patterson, G. D.; Matyjaszeswski, K. *Macromolecules* **2003**, *36*, 5094−5104.
(4) Carrot, G.; Diamanti, S.; Manuszak, M.; Charleux, B.; Vairon, J.-P. *J. Polym. Sci., Part A: Polym. Chem.* **2001**, *39*, 4294−4301.
(5) Husseman, M.; Malmstrom, E. E.; McNamara, M.; Mate, M.; Mecerreyes, D.; Benoit, D. G.; Hedrick, J. L.; Mansky, P.; Huang, E. Russel, T. P.; Hawker, C. J. *Macromolecules* **1999**, *32*, 1424−1429.
(6) Carrot, G.; Rutot-Houze, D.; Pottier, A.; Degee, P.; Hilborn, J.; Dubois, P. *Macromolecules* **2002**, *35*, 8400−8404.
(7) Le, T. P.; Moad, G.; Rizzardo, E.; Thang, S. H. PCT Int. Appl. WO 9801478, 1998.
(8) Monteiro, M. J.; de Brouwer, H. *Macromolecules* **2001**, *34*, 349−352.
(9) Kanagasabapathy, S.; Sudalai, A.; Benicewicz, B. C. *Macromol. Rapid Commun.* **2001**, *22*, 1076−1080.
(10) Mayadunne, R. T. A.; Jeffery, J.; Moad, G.; Rizzardo, E. *Macromolecules* **2003**, *36*, 1505−1513.
(11) Li, C.; Benicewicz, B. C. *J. Polym. Sci., Part A: Polym. Chem.* **2005**, *43*, 1535−1543.

(12) Mitsukami, Y.; Donovan, M. S.; Lowe, A. B.; McCormick, C. L. *Macromolecules* **2001**, *34*, 2248−2256.
(13) Baum, M.; Brittain, W. J. *Macromolecules* **2002**, *35*, 610−615.
(14) Tsujii, Y.; Ejaz, M.; Sato, K.; Goto, A.; Fukuda, T. *Macromolecules* **2001**, *34*, 8872−8878.
(15) Raula, J.; Shan, J.; Nuopponen, M.; Niskanen, A.; Jiang, H.; Kauppinen, E. I.; Tenhu, H. *Langmuir* **2003**, *19*, 3499−3504.
(16) Skaff, T.; Emrick, T. *Angew. Chem., Int. Ed.* **2004**, *43*, 5383−5386.
(17) Li, C.; Benicewicz, B. C. *Macromolecules* **2005**, *38*, 5929−5936.
(18) Chong, Y. K.; Krstina, J.; Le, T. P. T.; Moad, G.; Postma, A.; Rizzardo, E.; Thang, S. H. *Macromolecules* **2003**, *36*, 2256−2272.
(19) Kjaer, A. *Acta Chem. Scand.* **1952**, *6*, 327−332.
(20) Kjaer, A. *Acta Chem. Scand.* **1952**, *6*, 1374−1383.
(21) Thomas, T. B.; Convertine, A. J.; Hester, R. D.; Lowe, A. B.; McCormick, C. L. *Macromolecules* **2004**, *37*, 1735−1741.
(22) Greenwald, R. B.; Pendri, A.; Martinez, A.; Gilbert, C.; Bradley, P. *Bioconjugate Chem.* **1996**, *7*, 638−641.
(23) Perrier, S.; Barner-Kowollik, C.; Quinn, J. F.; Vana, P.; Davis, T. P. *Macromolecules* **2002**, *35*, 8300−8306.
(24) Vana, P.; Davis, T. P.; Barner-Kowollik, C. *Macromol. Theory Simul.* **2002**, *11*, 823−835.
(25) de Brouwer, J. A. M.; Schellekens, M. A. J.; Klumperman, B.; Monteiro, M. J.; German, A. L. *J. Polym. Sci., Part A: Polym. Chem.* **2000**, *19*, 3596−3603.
(26) McLeary, J. B.; Calitz, F. M.; McKenzie, J. M.; Tonge, M. P.; Sanderson, R. D.; Klumperman, B. *Macromolecules* **2004**, *37*, 2383−2394.
(27) Coote, M. L. *Macromolecules* **2004**, *37*, 5023−5031.
(28) Feldermann, A.; Coote, M. L.;Stenzel, M. H.; Davis, T. P.; Barner-Kowollik, C. *J. Am. Chem. Soc.* **2004**, *126*, 15915−15923.
(29) Barner-Kowollik, C.; Quinn, J. F.; Morsley, D. R.; Davis, T. P. *J. Polym. Sci., Part A: Polym. Chem.* **2001**, *39*, 1353−1365.
(30) Vana, P.; Quinn, J. F.; Davis, T. P.; Barner-Kowollik, C. *Aust. J. Chem.* **2002**, *55*, 425−431.
(31) Chen, R. Ph.D. Thesis, Rensselaer Polytechnic Institute, 2003.

MA051983T